JOURNAL OF MATERIALS SCIENCE 33 (1998) 3267–3273

Influence of a transition metal oxide (CuO) on the superplastic behaviour of 8 mol % yttria-stabilised cubic zirconia polycrystal (8Y-CSZ)

S. TEKELI, T. I. DAVIES
Materials Science Centre, University of Manchester/UMIST, Grosvenor Street, Manchester, MI 7HS, UK

The microstructure and superplastic deformation of fine-grained undoped 8Y-CSZ and 1 wt % CuO doped 8Y-CSZ have been investigated in tension in the temperature range 1503 to 1623 K and strain rate range 5×10^{-5} to 1×10^{-3} s^{-1}. Deformation of the undoped 8Y-CSZ was characterized by large strain-hardening with limited tensile elongations of 20%; this was mainly due to severe grain growth during deformation. The addition of a small amount of a transition metal oxide (CuO) resulted in a decrease in strain-hardening and enhanced tensile elongations up to 78%. The ductility enhancement in the CuO doped 8Y-CSZ was due to copper segregation to grain boundaries, thus facilitating grain boundary sliding. In addition, the enhanced ductility in the doped material was related to a reduction in flow stress which, in turn, suppressed cavitation and delayed fracture. © *1998 Kluwer Academic Publishers*

1. Introduction

Superplasticity in fine-grained ceramics has been extensively studied in recent years. Large tensile elongations have been found in many ceramics and ceramic composites such as yttria-stabilized zirconia [1, 2], alumina [3, 4], hydroxyapatite [5], zirconia–alumina [6, 7], mullite–zirconia [8], silicon carbide [9], silicon nitride–silicon carbide [10, 11] and iron–iron carbide [12]. Of the above materials, tetragonal zirconia (TZP) has been intensively investigated, beginning with the work of Wakai *et al.* [1] in which a tensile elongation to failure of 100% at 1723 K was obtained. In the ensuing years, tensile ductility in the same material has been improved and Kajihara *et al.* [13] have reported an elongation to failure of 1038% in 2.5Y-TZP containing 5 wt % SiO_2 at 1673 K and at 1.3×10^{-4} s^{-1}. In contrast, such elongations have not been obtained in cubic zirconia despite attempts to attain the high temperature ductility [14]. As stated by Chen and Xue [14] microstructural superplasticity requires an ultra fine grain size that is stable against coarsening during sintering and high temperature deformation. A low sintering temperature is a necessary, but not a sufficient, condition for achieving the required microstructure. In many cases, it seems that the selection of an appropriate crystalline phase is also crucial for obtaining an ultra fine grain size, for instance, tetragonal zirconia is superplastic whereas cubic zirconia is not [14]. Extensive ductilities in tetragonal zirconia is a consequence of grain size stability during high temperature deformation; this grain size stability is associated with the segregation of solute cations to grain boundaries, which lowers grain boundary mobility and grain boundary energy, thus increasing the cohesive strength of the grain boundary. Compared to tetragonal zirconia, cubic zirconia suffers fast grain growth and has only limited cation segregation at grain boundaries; consequently, cubic zirconia has a lower grain boundary cohesive strength and a higher grain boundary energy.

In the present study, preliminary results are given for superplastic deformation in fine-grained undoped 8Y-CSZ and 1 wt % CuO doped 8Y-CSZ tested at various temperatures and strain rates.

2. Experimental procedure

The starting material was a fine-grained 8 mol % yttria-stabilized cubic zirconia (8Y-CSZ) with an average grain size of 0.3 μm, supplied by Mandoval Ltd. (Zirconia Sales Ltd.) This powder was used in two conditions: a) as-received without an added dopant and b) 1 wt % CuO doped 8Y-CSZ. CuO was produced from analytical grade $Cu(NO_3)_2 3H_2O$. Introducing the metal oxide (CuO) to 8Y-CSZ was achieved by adding an appropriate amount of an aqueous solution of $Cu(NO_3)_2 3H_2O$ to a dispersed suspension of cubic zirconia in distilled water. This slurry was ball milled for 60 min using zirconia balls and flocculated by the addition of ammonia. The flocculated mixture was then dried at 373 K overnight and calcined in air at 973 K for 30 min.

A slip casting method was used for the preparation of tensile specimens; this method allowed the

economical production of net shapes that required no machining. The slip casting slurry was prepared by dispersing the powder (68 wt %) in distilled water with a dispersing agent (Dispex A40); the slurry was then wet ball milled for 4 h to obtain a good dispersion. The milled slurry was injected by a syringe into a plaster mould. Cast specimens were released from the mould after ~7 min and then air dried at ~25 °C for a few days. These specimens were presintered at 1123 K to make them more handleable and smooth surfaces were obtained by carefully grinding off any casting protrusions. Specimens were then pressureless sintered in air at 1623 K for 30 min; specimens with ~95% of theoretical density were regularly produced [15, 16]. Density measurements were made by the Archimedes displacement method.

High temperature uniaxial tensile tests were carried out in air using an Instron 4505 testing machine. A single zone vertical split furnace (supplied by Carbolite Furnaces Ltd.) with molybdenum disilicide elements was mounted on the crosshead of the test frame; tensile load was applied using high density sintered alumina rods in a pin loading mechanism. Careful specimen alignment was essential to avoid fracture on loading. After achieving the desired (uniform) test temperature, usually at a heating rate of 423 K h^{-1}, the assembly was held at that temperature for ~10 min. A small tensile load was then applied on the specimen as a pre-load and the alignment checked before testing. Deformation was continuously monitored using a computerized system equipped with a data acquisition facility that allowed tests to be controlled under a constant strain rate.

Scanning electron microscopy (SEM 525) and analytical transmission electron microscopy (EM 430T) were used to characterize the microstructure of the as-sintered and deformed samples. Microchemical analyses were carried out using an EDAX 9900 microanalyser attached to the EM 430T.

3. Experimental results and discussion

Table I shows the relative densities of undoped and CuO-doped 8Y-CSZ, sintered at different temperatures for 1 h. For undoped 8Y-CSZ a maximum density of 99% was obtained at 1773 K whereas the same density for CuO-doped 8Y-CSZ was achieved at 1623 K. This lower sintering temperature in the presence of the dopant probably indicates the action of an activated species at grain boundaries. (It is known that a eutectic composition exists at about 1363 K to 1403 K in the system of CuO/CuO-ZrO_2 [17] depending on the oxygen potential.)

Comparison of the grain sizes of the two alloys sintered at the same temperature, Fig. 1, indicates a smaller average grain size in undoped 8Y-CSZ (1.45 μm) than in CuO-doped 8Y-CSZ (1.65 μm). The grains were regular in shape and the pores were mainly at grain boundaries.

3.1. Superplastic behaviour

Specimens of CuO-doped 8Y-CSZ tested at a strain rate of 1×10^{-4} s^{-1} and 1623 K exhibited elongations to failure of ~78%, whereas elongation to failure in undoped 8Y-CSZ was limited and a maximum elongation of ~20% was obtained for the above testing conditions.

The true stress–true strain curves for undoped and CuO-doped 8Y-CSZ are shown in Figs 2 and 3 for a range of temperatures and strain rates, respectively.

True stress–true strain curves of the undoped 8Y-CSZ were characterized by large strain hardening followed by early fracture after reaching a peak stress; the flow stress increased with increasing strain rate and decreasing temperature. The cause of low superplastic ductility and high strain hardening is related to extensive grain growth which migrates against grain boundary sliding, causing early fracture.

The CuO-doped 8Y-CSZ showed less strain hardening and larger elongations; the flow stress was again seen to increase with increasing strain rate and decreasing temperature. The reduction of flow stress and ductility increase are probably due to the effect of copper on the grain boundary mobility and ease of grain boundary sliding.

The logarithmic relationship between flow stress and strain rate for undoped 8Y-CSZ and CuO-doped 8Y-CSZ is plotted in Fig. 4 over a range of temperature; the experimental data fall on straight lines. The values of strain rate sensitivity calculated from the slope of Fig. 4 are in the range 0.4 to 0.51, which increases slightly with increasing temperature and with addition of CuO.

The relationship between strain rate and reciprocal of absolute temperature at 20 MPa is shown in Fig. 5; the experimental data gave good-fit straight line relationships. The activation energies calculated were 510 ± 40 kJ mol^{-1} for undoped 8Y-CSZ and 480 ± 25 kJ mol^{-1} for CuO-doped 8Y-CSZ. Similar values of Q have been reported for high temperature plastic deformation of cubic [18, 19] and tetragonal [20] zirconia polycrystals doped with Y_2O_3. The slightly lower activation energy (and larger elongation) in the CuO-doped 8Y-CSZ may indicate that grain boundary sliding is facilitated by an (unidentified) interface reaction at the dopant/grain interface.

TABLE I Relative (theoretical) densities of undoped and CuO-doped 8Y-CSZ, sintered at various temperatures for 1 h.

	Sintering temperature (K)	1223	1373	1423	1473	1523	1573	1623	1673	1773
Relative density	Undoped 8Y-CSZ	–	50.4	–	66.4	–	94.5	–	98.9	99.9
	CuO-doped 8Y-CSZ	55.7	–	77.1	–	90.9	97.5	99.9	–	–

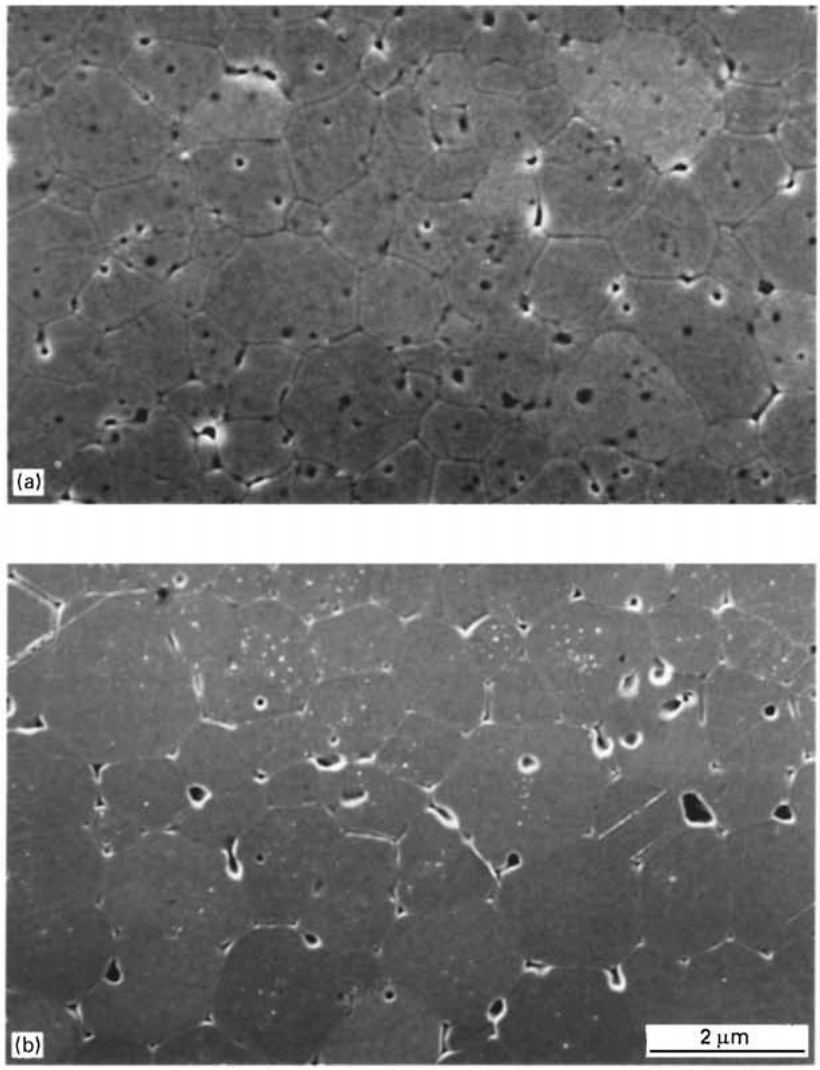

Figure 1 SEM micrographs of a) undoped 8Y-CSZ and b) 1 wt % CuO-doped 8Y-CSZ, sintered at 1573 K for 1 h. Relative densities were 94.5% for (a) and 97.5 for (b), respectively.

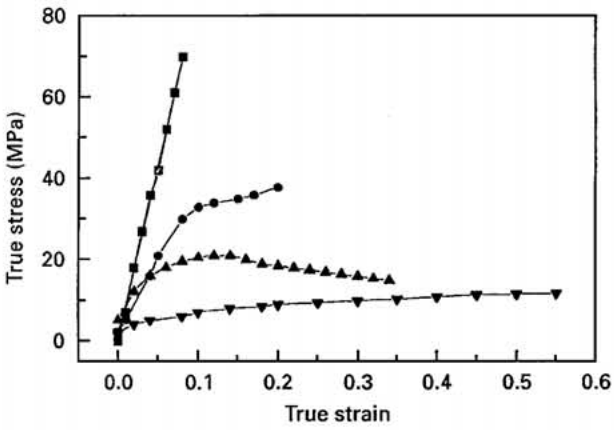

Figure 2 True stress–true strain relationships of undoped ((■) 1503 K, (●) 1623 K) and CuO doped ((▲) 1503 K, (▼) 1623 K) 8Y-CSZ deformed at various temperatures and $1 \times 10^{-4} s^{-1}$, showing the effect of temperature on flow stress.

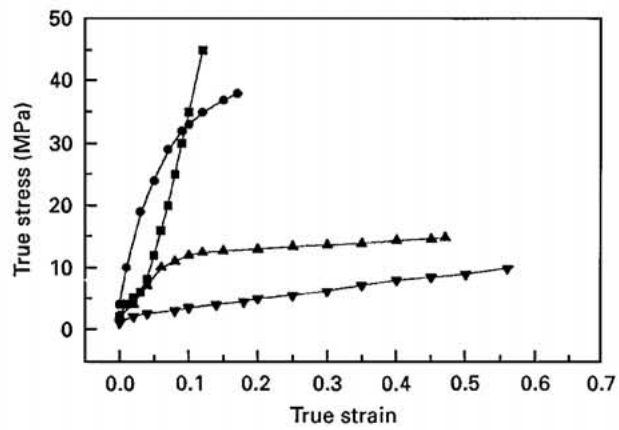

Figure 3 True stress–true strain relationships of undoped ((■) $1 \times 10^{-4} s^{-1}$, (●) $5 \times 10^{-3} s^{-1}$) and CuO doped ((▲) $1 \times 10^{-4} s^{-1}$, (▼) $5 \times 10^{-5} s^{-1}$) 8Y-CSZ deformed at various strain rates and at 1573 K, indicating the effect of strain rate on flow stress.

3.2. Microstructural observation

It has been suggested that to enhance grain boundary diffusivity and to lower deformation resistance in zirconia ceramics, additives which segregate to the grain boundary and form a low-melting phase could be effective [14]; this grain boundary phase would act to reduce the friction between grains, promoting grain boundary sliding and allowing an enhancement in strain rate [21].

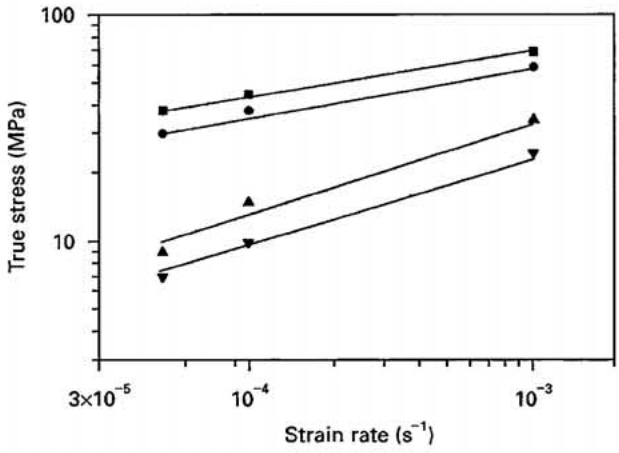

Figure 4 True stress–true strain relationships for undoped ((■) 1573 K, $m = 0.4$, (●) 1623 K, $m = 0.41$) and CuO doped ((▲) 1573 K, $m = 0.49$, (▼) 1623 K, $m = 0.51$) 8Y-CSZ deformed at various strain rates and temperatures.

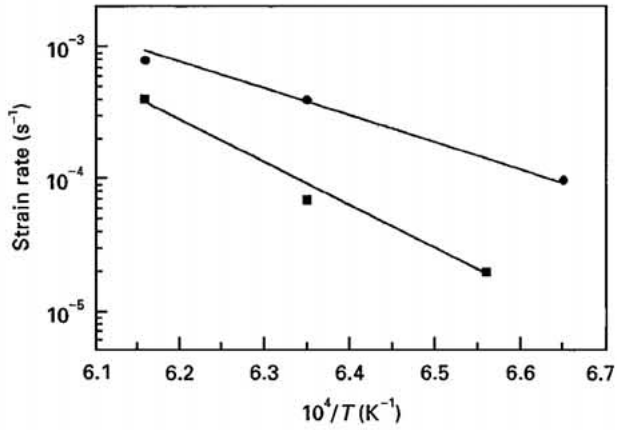

Figure 5 Log strain rate versus reciprocal temperature showing the activation energies in undoped ((■) $Q = 510 \pm 40\,\mathrm{kJ\,mol^{-1}}$) and CuO doped ((●) $Q = 480 \pm 45\,\mathrm{kJ\,mol^{-1}}$) 8Y-CSZ.

Substantial TEM work was carried out to examine grain boundaries and to detect traces of additional species at grain boundaries or triple points. Superplastically deformed undoped 8Y-CSZ samples showed a well-defined grain structure with grains having an essentially hexagonal/pentagonal cross-section with sharp apices. A typical microstructure is shown in Fig. 6a for a specimen elongated 20% at 1623 K and

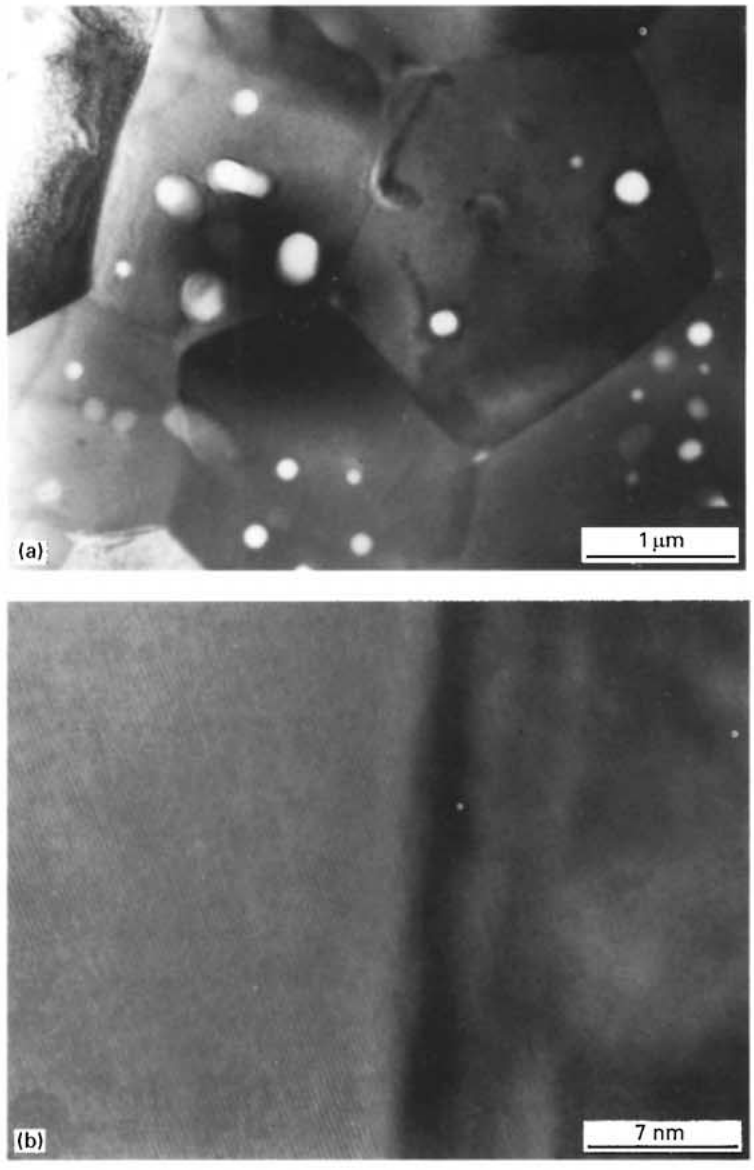

Figure 6 Transmission electron micrograph of undoped 8Y-CSZ specimen deformed at 1623 K and $1 \times 10^{-4}\,\mathrm{s^{-1}}$ ($e_f = 20\%$) and b) a high resolution transmission electron micrograph of a grain boundary in the same material.

$1 \times 10^{-4}\,s^{-1}$. The grains were equiaxed and dislocation free; there was no evidence of grain elongation. A high resolution image of a grain boundary from the same sample is shown in Fig. 6b. No separate grain boundary phase was detected at either triple points or on the grain boundaries; there was good coherency and lattice matching between grains.

A TEM micrograph of 8Y-CSZ + 1 wt % CuO is shown in Fig. 7 together with the corresponding X-ray spectra; the sample had been elongated 78% at 1623 K and $1 \times 10^{-4}\,s^{-1}$. Small, but well defined, amounts of grain boundary phase (indicated by the arrow Fig. 7a) were regularly found at grain boundaries, although there was no evident accumulation of the dopant at grain boundary triple points. EDS microanalysis, using a nanoprobe, of several grain boundary regions showed that the boundary phase was Cu-rich, relative to the interior of the grains; this grain boundary region also contained traces of yttrium. The relative Cu concentrations in the matrix and the grain boundary region were quantitatively evaluated using an EDAX. Measurements were made by traversing from the grain boundary region towards the grain interior at 5 successive steps of 0.2 μm each. The results, Fig. 8, identify a segregation of copper to grain boundary regions.

In the light of the above results it is deduced that the copper oxide dopant segregates to and concentrates on grain boundaries: this is considered to enhance superplastic ductility by facilitating grain boundary sliding (the flow stress is also slightly lower). Also, the presence of the dopant at grain boundaries may help to reduce residual stresses in the material by allowing grain rearrangement to occur more easily. As a result, these grain boundaries would be expected to have reasonable strength and good cavitation resistance.

3.3. Deformation characteristics

High temperature deformation is often expressed by the equation

$$\dot{\varepsilon} = A\sigma^n d^{-p} \exp(-Q/RT) \qquad (1)$$

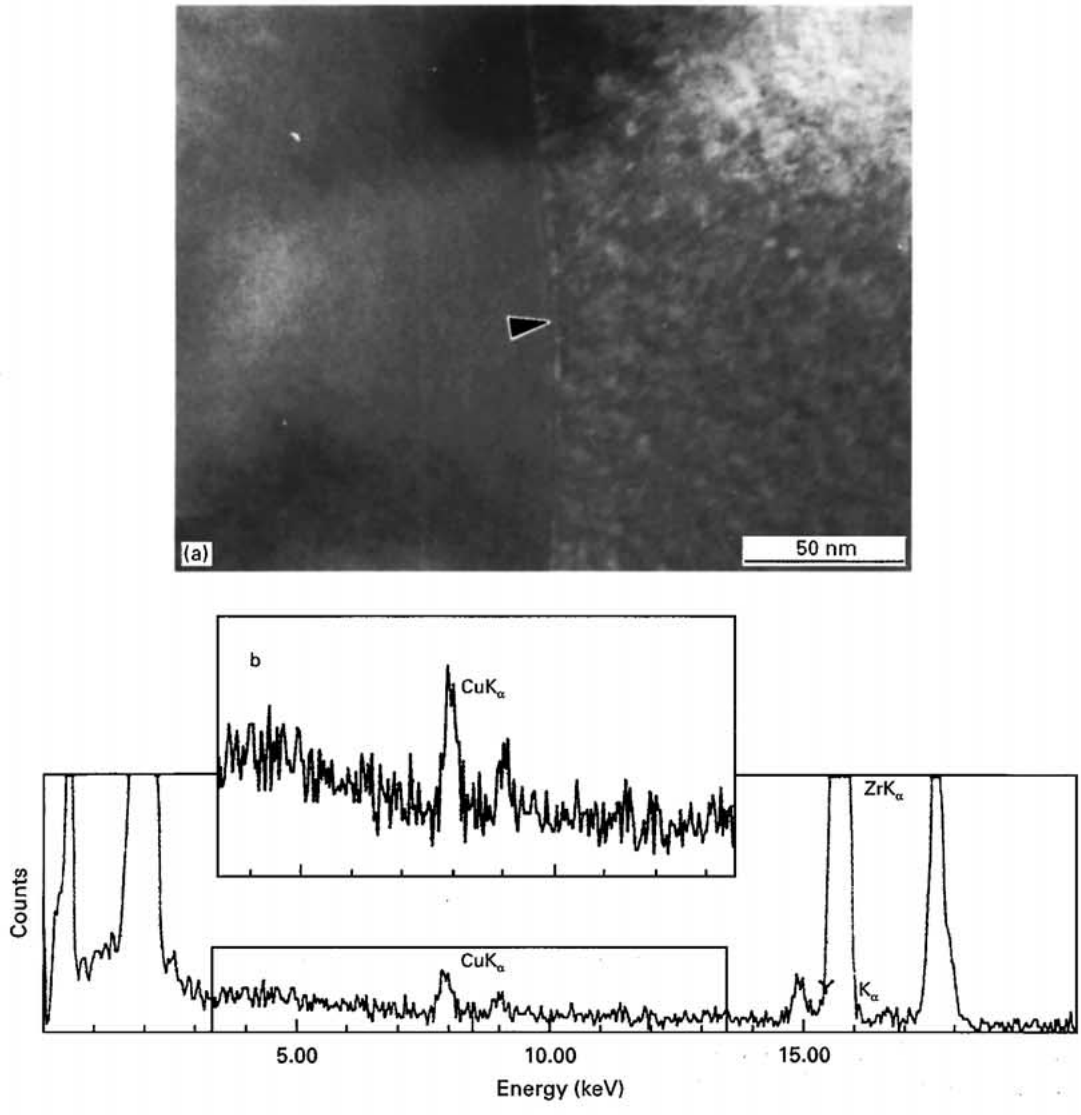

Figure 7 Transmission electron micrograph revealing a thin, continous layer of boundary segregation in superplastically deformed 8Y-CSZ doped with 1 wt % CuO ($T = 1623\,K$, $\varepsilon = 1 \times 10^{-4}\,s^{-1}$, $e_f = 78\%$) and b) the corresponding X-ray spectra at the grain boundary (marked by the arrow in (a)) showing the Cu-rich phase (enlarged inset)

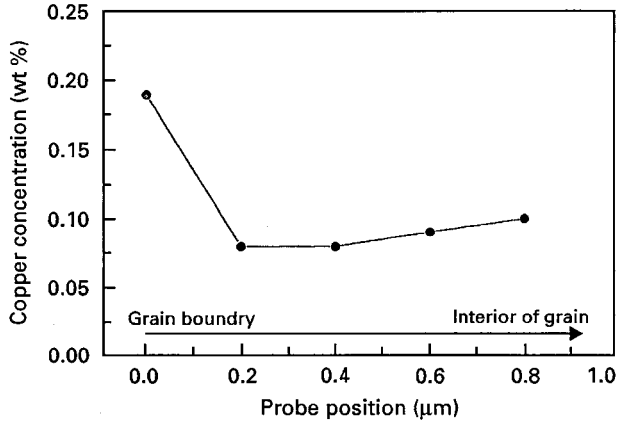

Figure 8 Weight percentage of copper in a grain boundary scan in doped 8Y-CSZ, (determined by EDS).

where A is a material constant, σ is the stress for deformation, n is a stress exponent, d is grain size, p is a grain size exponent, T is absolute temperature, Q is an activation energy for the deformation process and R is the gas constant.

A number of mechanisms have been proposed to describe the deformation of cubic zirconia, namely; a) dislocation creep; in single-crystal 9.4 mol % yttria-stabilized cubic zirconia tested in the temperature range of 1573 to 1823 K, an activation energy of $600\,kJ\,mol^{-1}$ and an n value of 4.5 were obtained; it was proposed that deformation was due to diffusive recovery (dislocation climb) [22] ; b) diffusion creep; in coarse grained 25 mol % yttria stabilized cubic zirconia [23] tested in the temperature range 1673 to 1873 K, it was claimed that an activation energy of $550\,kJ\,mol^{-1}$ and a measured grain size exponent of $p = 2.2 \pm 0.2$ demonstrated that creep occurred by a Nabarro–Herring mechanism. This conclusion was supported by the observation that grains in deformed samples remained dislocation free and equiaxed. In both cases, the creep activation energy was considered to be associated with the slower cation diffusion.

The present results suggest that it is difficult to relate the experimental stress exponent of 2 to an intragranular dislocation creep mechanism, because the grain elongation after deformation was experimentally observed to be negligible and the transmission electron microscopy studies did not show any intragranular dislocation activity. A stress exponent of 2 and the lack of grain elongation is also inconsistent with lattice diffusion as the primary deformation process. By elimination of these deformation mechanisms, it is deduced that the most likely possible deformation mechanism for both undoped and doped 8Y-CSZ is consistent with grain boundary sliding accommodated by a hitherto undefined interface reaction. The similarity in behaviour of the undoped and doped 8Y-CSZ indicates that the fundamental mechanism of superplasticity is unaffected by the addition of the transition metal oxide, although the total elongation is increased and the flow stress reduced.

4. Conclusion

1) The addition of CuO enhanced both densification and grain growth in 8Y-CSZ.

2) For undoped 8Y-CSZ, stress–strain curves were characterized by large strain hardening followed by early fracture with low ductilities. The maximum elongation observed was 20% at 1673 K and $1 \times 10^{-4}\,s^{-1}$, whereas, with the addition of a small amount of the transition metal oxide (CuO) to 8Y-CSZ, strain hardening was reduced and tensile ductility was increased to 78% for the same test conditions.

3) The m (strain rate sensitivity) values determined from $\log \sigma$–$\log \varepsilon$ were between 0.4 and 0.51. The addition of a small amount of a transition metal oxide (CuO) to 8Y-CSZ slightly increased the value of the strain rate sensitivity.

4) The activation energies associated with superplastic deformation were $510 \pm 40\,kJ\,mol^{-1}$ for undoped 8Y-CSZ and $480 \pm 45\,kJ\,mol^{-1}$ for doped 8Y-CSZ. In this latter case the presence of either a faster, easier diffusion path at grain boundaries or the creation of an interface reaction at the grain boundaries, that allowed grain boundary sliding to operate at a lower stress, facilitated larger elongations.

5) TEM studies of deformed 8Y-CSZ with and without CuO addition revealed that in undoped 8Y-CSZ no distinct phase separation was observed either at triple points or along grain boundaries, whereas in doped 8Y-CSZ, a continuous intergranular segregation of dopant of a fairly uniform thickness existed. It is proposed that this segregation of dopant at grain boundaries facilitated grain boundary sliding and minimized residual stresses by allowing grain rearrangement and rotation.

6) The stress exponent of approximately 2, the retention of equiaxed grains during deformation and values of experimental activation energies for the deformation indicate that grain boundary sliding accommodated by (an undefined) interface reaction is the most likely mechanism of superplastic flow in 8Y-CSZ. Addition of a transition metal oxide (CuO) did not change the deformation mechanism but facilitated elongation and lowered the flow stress.

Acknowledgements

The authors wish to express their gratitude to the University of Gazi, Turkey, for financial support for one of us (S. T.) and to the Manchester Materials Science Centre for the provision of laboratory facilities.

References

1. F. WAKAI, S. SAKAGUCHI and Y. MATSUN, *Adv. Ceram. Mater.* **1** (1986) 259.
2. F. WAKAI, S. SAKAGUCHI, K. KANAYAMA, H. KATO and H. ONISHI, "Ceramic Materials and Components for Engines" (Deutsehe Keramische Gesellschaft, Bad Honnet, 1986) p. 315.
3. W. R. CANON, W. H. RHODES and A. H. HEUER, *J. Am. Ceram. Soc.* **63** (1980) 46.
4. Z. C. WANG, T. J. DAVIES, N. RIDLEY and A. A. OGWU, *Acta Mater.* **44** (1996) 4301.

5. F. WAKAI, Y. KODAMA, S. SAKAGUCHI and T. NONAMI, *J. Am. Ceram. Soc.* **73** (1990) 257.
6. F. WAKAI and H. KATO, *Adv. Ceram. Mater.* **3** (1988) 71.
7. T. G. NIEH, C. M. McNALLY and J. WADSWORTH, *Scr. Metall.* **23** (1987) 457.
8. C. K. YOON and W. I. CHEN, *J. Am. Ceram. Soc.* **73** (1990) 1555.
9. C. CARRY and A. MOCELLIN, "Deformation of Ceramics II" (Plenum, New York, 1984) p. 391.
10. F. WAKAI, Y. KODAMA, S. SAKAGUCHI, K. MURAYAMA, K. IZAKI and K. NIIHARA, *Nature* **344** (1990) 421.
11. T. ROUXEL, F. WAKAI and K. IZAKI, *J. Am. Ceram. Soc.* **75** (1992) 2363.
12. W. J. KIM, J. WOLFENSTINE, G. FROMMEYER and O. D. SHERBY, *Scr. Metall.* **23** (1989) 1515.
13. K. KAJIHARA, Y. YOSHIZAWA and T. SAKUMA, *ibid.* **28** (1993) 559.
14. I. W. CHEN and L. A. XUE, *J. Am. Ceram. Soc.* **73** (1990) 2585.
15. S. TEKELI, PhD Thesis, The University of Manchester and UMIST (1996).
16. Z. C. WANG, T. J. DAVIES and N. RIDLEY, *Scr. Metall. Mater.* **28** (1993) 301.
17. A. M. M. GADALA and J. WHITE, *J. Am. Ceram. Soc.* **52** (1969) 33.
18. M. S. SELTER and P. K. TALTY, *ibid.* **58** (1975) 124.
19. D. DIMOS and D. L. KOHLSTEDT, *ibid.* **70** (1987) 531.
20. F. WAKAI and T. J. NAGONA, *Mater. Sci.* **26** (1991) 241.
21. M. F. ASHBY, *Acta Metall.* **31** (1953) 129.
22. J. M. FERNANDEZ, M. J. MELENDO and A. P. RODRIGUES, *J. Am. Ceram. Soc.* **73** (1990) 2452.
23. D. DIMOS and D. L. KOHLSTEDT, *ibid.* **70** (1987) 531.

Received 23 June 1997
and accepted 7 April 1998